International Journal of Non-Linear Mechanics

Modeling and dynamic analysis of fractional order nonlinear viscoelastic rod

--Manuscript Draft--

Manuscript Number:	NLM-D-23-00681
Article Type:	Full Length Article
Keywords:	Nonlinear viscoelastic rod; Differential equation; Fractional order constitutive model; Numerical solution; Dynamic analysis
Corresponding Author:	Yajuan Hao Yanshan University CHINA
First Author:	Meihua Zhang
Order of Authors:	Meihua Zhang
	Yajuan Hao
	Yiming Chen
	Gang Cheng
	Thierry Barrière
	Jingguo Qu
Abstract:	A fractional order constitutive behavior law is proposed in this paper to describe the viscoelasticity of the nonlinear rod. The fractional governing equation of the nonlinear viscoelastic rod is established. An effective algorithm based on the shifted Legendre polynomials is used to solve the governing equation directly in the time domain. The effectiveness of the proposed numerical algorithm is confirmed by the convergence analysis. Its accuracy is verified by the comparison with the analytical solution of a dimensionless equation. The dynamic response of the viscoelastic rod under various loading conditions is analyzed. The influence of loading parameters on the dynamic characteristics of the rod is investigated according to the evolution of displacement and stress.
Funding Information:	National Natural Science Foundation of China (5207041692) — Yiming Chen
Suggested Reviewers:	Zhiqiang Feng zhiqiang.feng@univ-evry.fr
	André Langlet andre.langlet@univ-orleans.fr
	Jiaquan Xie xiejiaquan@tyut.edu.cn
	abel Cherouat abel.cherouat@utt.fr
	Sami holopainen sami.holopainen@tut.fi

Modeling and dynamic analysis of fractional order nonlinear viscoelastic rod

Meihua Zhang[a], Yajuan Hao[a,*], Yiming Chen[a,b], Gang Cheng[c], Thierry Barrière[d], Jingguo Qu[e]

[a] *School of Science, Yanshan University, Qinhuangdao 066004, China*
[b] *LE STUDIUM RESEARCH Professor, Loire Valley Institute for Advanced Studies, Orléans 45000, France*
[c] *INSA Centre Val de Loire, Univ. Tours, Univ. Orléans, LaMé, 3 rue de la chocolaterie, CS 23410, 41034 Blois, France*
[d] *Universit de Franche-Comté, CNRS, institut FEMTO-ST, F-25000 Besançon, France*
[e] *College of Science, North China University of Science and Technology, Tangshan 063000, China*

Abstract

A fractional order constitutive behavior law is proposed in this paper to describe the viscoelasticity of the nonlinear rod. The fractional governing equation of the nonlinear viscoelastic rod is established. An effective algorithm based on the shifted Legendre polynomials is used to solve the governing equation directly in the time domain. The effectiveness of the proposed numerical algorithm is confirmed by the convergence analysis. Its accuracy is verified by the comparison with the analytical solution of a dimensionless equation. The dynamic response of the viscoelastic rod under various loading conditions is analyzed. The influence of loading parameters on the dynamic characteristics of the rod is investigated according to the evolution of displacement and stress.

Keywords: Nonlinear viscoelastic rod, Differential equation, Fractional order constitutive model, Numerical solution, Dynamic analysis.

1. Introduction

Viscoelastic materials are widely applied in the fields of biology, physics and engineering [1; 2]. However, the mechanical behavior of viscoelastic materials is

*Corresponding author
Email address: `zmh@stumail.ysu.edu.cn` (Yajuan Hao)

significantly affected by various loading conditions. The mechanical behavior of viscoelastic materials changes with time [3; 4]. The viscoelasticity of the graphene reinforced polymer nanocomposites was investigated by using coarse-grained molecular dynamics [5]. The interfacial interactions between graphene and polymer affected the dynamic modulus of the nanocomposites, which improved the understanding of failure mechanisms of composite in nanoscale. The viscoelastic behaviors of loaded elastomers were modelling based on their experimental surfaces tensions [6]. The developed method permitted a numerical simulation for the dynamic moduli in filled elastomers.

In recent years, more and more attentions have been paid on the fractional calculus in the field of mathematic, physics and mechanical engineering [7–9]. The fractional order operator is an effective tool in describing the viscoelastic behavior, especially in establishing the time-varying model [10–13]. Fractional viscoelastic model is widely used because they can describe the behavior of viscoelastic materials with fewer parameters [14]. Denis et al. [15] proposed a hysteretic model using the fractional derivative to describe the mechanical behavior of fiber reinforced composites. The results indicated that it predicted more accurately the residual stress and plastic strain of the composites. Loghman et al. [16] employed a fractional order Kelvin-Voigt model to describe the viscoelasticity of the microbeam. The numerical results showed that the effects of the fractional derivative were considerable, especially when the amplitude of vibration was high.

Rod is considered to be an essential structure in aerospace, biomechanics and mechanical engineering [17–19]. Its dynamic behavior is considered as a main scientific issue to improve the accuracy of the numerical modeling. Alp et al. [20] solved the motion equation of the cycloidal rod in the Laplace domain by using the complementary function method to study their dynamic response in the damping and free vibration. Adhikari et al. [21] obtained the stiffness and mass matrix of the rod according to the conventional finite element method, and analyzed the free and forced axial vibration of the damped nonlocal rod. Mazur-Śniady et al. [22] researched the axial vibration of a finite period composite rod under two various moving random loads by using the perturbation method. Malara et al. [23] used the boundary element approach to solve the differential equation, and analyzed the response statistics of the fractional order rod under random excitation. Du et al. [24] proposed a unified model to describe the static equilibrium of the elastic rods with large deformations. A nonlinear optimization algorithm based on the total potential energy was introduced to effectively solve the equilibrium problem of the rod with various boundary conditions. Ausas et al. [25] used Cosserat rods to modelling one-dimensional solid with large deformations in Newtonian fluids. An active response was obtained for the planar non-shaearable solid according to the time dependent strain energy. Zhang [26] proposed a new high order finite difference method based on nonlocal elasticity theory to predict the axial vibration behavior of variable density elastic nanorods. Shakhlavi [27] used Galerkin and multi-scale methods to analyse the vibration characteristics of the viscoelastic rod with thermal environment.

Different from the above methods, fractional models possess memory characteristics and the advantages of less parameters and high accuracy. They have become the powerful mathematical modelling tools to describe the material mechanical behaviors [28–31]. Patnaik et al. [32] employed a fractional-order nonlocal model to study the static and dynamic response of plates with different loading and boundary conditions. Stefański [33] used fractional order model to describe the wave propagation and discussed the further application in electromagnetic cloaking. Javadi and Rahmanian [34] applied the fractional Kelvin-Voigt model to describe the viscoelastic behaviors of materials. The influence of parameters in the model on the resonance of the beam was analysed under various excitations. Cao et al. [35] analyzed the dynamic analysis of viscoelastic columns under different external loads and the stress and strain at different times based on the fractional order model. Dang and Chen [36] analyzed the dynamic characteristics of viscoelastic arch with variable cross section based on fractional order model. Sun et al. [37] numerically analyzed fractional order viscoelastic plates in the time domain, and also analyzed the effect of damping coefficient on their vibration amplitude.

Development of an effective numerical algorithme for obtaining the approximate solutions of fractional differential governing equations has become a main research issue. Ibraheem et al. [38] proposed an optimal variational iteration method to solve partial and ordinary fractional differential equations. Usman et al. [39] employed linearized sepctral and semi descrete methods to solve the fractional nonliear differential equation. The proposed method converted the highly nonlinear problems into a set of linear equations.

Orthogonal polynomials play an important role in solving fractional differential equations. Heydari et al. [40] used a numerical algorithm based on the Chebyshev polynomials to sovel the time fractional system. The proposed method transformed the fractional system into an algebraic system to approximate the unknown solution. Heydari et al. [41] solved a variable fractional order nonlinear coupled system based on shifted Legendre polynomials. Cao et al. [42] calculated the numerical solution of PMMA viscoelastic beam by using the shifted Legendre algorithm. Hesameddini and Shahbazi [43] solved the two-dimensional fractional integral equation using shifted Legendre polynomials. Hosseininia et al. [44] solved the extended Fisher Kolmogorov equation by using the shifted Legendre polynomial and the collocation method. The efficiency and accuracy of the shifted Legendre method are confirmed in the literature. In this paper, the shifted Legendre polynomials is employed to solve the fractional governing equations of the viscoelastic rod.

In this paper, a numerical algorithm based on shifted Legendre polynomials is used to obtain the approximate solutions of the fractional governing equation of nonlinear viscoelastic rod. The solutions are obtained directly in the time domain. Convergence analysis is performed to verify the effectiveness of the proposed algorithm. The evolution of the displacement of the viscoelastic rod under different loading conditions is analysed. The influence of loading parameters on its dynamic characteristics is investigated.

Section 2 introduces the definitions and characters of Caputo derivative and fractional order derivative. In section 3, the fractional order constitutive equation is used to establish the differential equation for the fractional order nonlinear viscoelastic rod. Section 4 presents the definition of shifted Legendre polynomials and deduces the differential operator matrix. In section 5, the convergence analysis is given, the numerical solution of a dimensionless equation is obtained, and compared with the analytical solution. In section 6, the dynamic characteristics of viscoelastic rod are studied and discussed. Section 7 is the conclusion of the research work.

2. Caputo fractional order derivative

In the section, the definition and some properties of Caputo fractional order derivative are given.

Definition 1: Caputo fractional order derivative [15]

$$D_x^\alpha f(x) = \begin{cases} \frac{d^m f(x)}{dx^m}, & \alpha = m \in N^+ \\ \frac{1}{\Gamma(m-\alpha)} \int_0^x \frac{f^{(m)}(y)}{(x-y)^{\alpha-m+1}} dy, & 0 < m-1 < \alpha < m \end{cases} \tag{1}$$

where α is fractional order derivative, $0 < \alpha < 1$, the function $f(x)$ is continuous, $\Gamma(*)$ is the Gamma function

$$\Gamma(z) = \int_0^\infty e^{-x} x^{z-1} dx \tag{2}$$

By this definition, the following formula is obtained

$$D_x^\alpha x^n = \begin{cases} \frac{\Gamma(n+1)}{\Gamma(n+1-\alpha)} x^{n-\alpha}, & n = 1, 2, ... \\ 0, & n = 0 \end{cases} \tag{3}$$

The properties of Caputo fractional order derivative are

$$D_x^\alpha C = 0 \tag{4}$$

$$D_x^\alpha [\mu f(x) + \xi g(x)] = \mu D_x^\alpha f(x) + \xi D_x^\alpha g(x) \tag{5}$$

where C, μ and ξ are constants.

3. Equation of motion

The fractional order model is applied to describe the stress-strain relationship of the viscoelastic rod [45]:

$$\sigma(x,t) = E_1 \varepsilon(x,t) + E_2 D_t^\alpha \varepsilon(x,t) \tag{6}$$

E_1 and E_2 are instant and prolonged elasticity modulus, respectively, D_t^α is α fractional order operator defined by Caputo, $\sigma(x,t)$ and $\varepsilon(x,t)$ are stress and strain respectively.

The relationship between strain and axial displacement is

$$\varepsilon(x,t) = \frac{\partial w(x,t)}{\partial x} \tag{7}$$

The viscoelastic rod under external load is shown in Fig. 1. Where l is the length of the rod, $f(x,t)$ is the external load, and $w(x,t)$ is the axial displacement. Based on Ref. [23], the differential equation of fractional order nonlinear viscoelastic rod under excitation load is obtained

$$\rho\frac{\partial^2 w(x,t)}{\partial t^2} - E_1\frac{\partial^2 w(x,t)}{\partial x^2} - E_2 D_t^\alpha \frac{\partial^2 w(x,t)}{\partial x^2} + c_0\rho w(x,t) + c_1\rho w^3(x,t) = f(x,t) \tag{8}$$

ρ is volumetric mass density, c_0 and c_1 are the characteristic parameters of Winkler-kind loads.

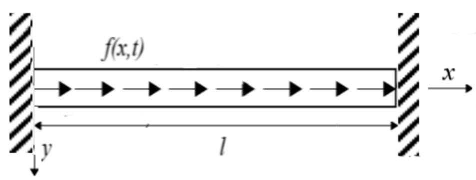

Fig. 1. Viscoelastic rod under external load.

Boundary conditions

$$w\,(0,t) = w\,(l,t) = 0 \tag{9}$$

Initial conditions

$$w(x,0) = \tfrac{\partial w(x,0)}{\partial t} = 0 \tag{10}$$

4. Numerical algorithm

In this part, the numerical solution to the fractional differential equation is obtained using the shifted Legendre polynomials algorithm. The differential operators of polynomials with integral and fractional orders are represented.

4.1. Polynomials definition

Definition 2: The shifted Legendre polynomials of n-order on $[0,1]$ is [46]

$$l_{n,k}(x)=\sum_{k=0}^{n}(-1)^{n+k}\frac{\Gamma(n+k+1)}{\Gamma(n-k+1)(\Gamma(k+1))^2}x^k \tag{11}$$

where $k=0,1,2,...,n$.

Let $\phi(x)$ represent a matrix consisting of a series of shifted Legendre polynomials, which can be expressed as

$$\phi(x)=[l_{n,0}(x),l_{n,1}(x),...l_{n,n}(x)]^T=AH(x) \tag{12}$$

where $H(x)=[1,x,...,x^n]^T$,

$$A=[a_{jk}]_{j,k=0}^{n},a_{jk}=\begin{cases}(-1)^{j+k}\frac{\Gamma(j+k+1)}{\Gamma(j-k+1)(\Gamma(j+1))^2},j\geq k\\ 0, \qquad\qquad\qquad\qquad j<k\end{cases} \tag{13}$$

By extending the shifted Legendre polynomials from the interval $[0,1]$ to the interval $[0,S]$, and the expression is

$$\begin{aligned}L_{n,k}(x)&=\sum_{k=0}^{n}(-1)^{n+k}\frac{\Gamma(n+k+1)}{\Gamma(n-k+1)(\Gamma(k+1))^2}(\tfrac{x}{S})^k\\&=\sum_{k=0}^{n}(-1)^{n+k}\frac{\Gamma(n+k+1)}{\Gamma(n-k+1)(\Gamma(k+1))^2}(\tfrac{1}{S})^k x^k\end{aligned} \tag{14}$$

where $k=0,1,2,...,n$.

Therefore, $\phi(x)$ can be converted to

$$\phi(x)=UH(x) \tag{15}$$

where $U=[u_{jk}]_{j,k=0}^{n},u_{jk}=\begin{cases}(-1)^{j+k}\frac{\Gamma(j+k+1)}{\Gamma(j-k+1)(\Gamma(j+1))^2}(\frac{1}{S})^j j\geq k\\ 0, \qquad\qquad\qquad\qquad j<k\end{cases}$

Similarly

$$\begin{aligned}L_{n,k}(t)&=\sum_{k=0}^{n}(-1)^{n+k}\frac{\Gamma(n+k+1)}{\Gamma(n-k+1)(\Gamma(k+1))^2}(\tfrac{x}{K})^k\\&=\sum_{k=0}^{n}(-1)^{n+k}\frac{\Gamma(n+k+1)}{\Gamma(n-k+1)(\Gamma(k+1))^2}(\tfrac{1}{K})^k t^k\end{aligned} \tag{16}$$

where $k=0,1,2,...,n$.

$$\phi(t)=VH(t) \tag{17}$$

where $t\in[0,\mathrm{K}]$, $H(t)=[1,t,...,t^n]^T$

$$V=[v_{jk}]_{j,k=0}^{n},v_{jk}=\begin{cases}(-1)^{j+k}\frac{\Gamma(j+k+1)}{\Gamma(j-k+1)(\Gamma(j+1))^2}(\frac{1}{K})^j,j\geq k\\ 0, \qquad\qquad\qquad\qquad j<k\end{cases} \tag{18}$$

4.2. Displacement function approximation

The displacement function $w(t)$ is continuous in $[0, K]$, the approximation of $w(t)$ by shifted Legendre polynomials is

$$w(t) \approx w_n(t) = \sum_{k=0}^{n} b_k L_{n,k}(t) = B^T \phi(t) \tag{19}$$

where $B^T = [b_0, b_1, ..., b_n]$. That

$$B^T \left\langle \phi(t), \phi^T(t) \right\rangle = \left\langle w(t), \phi^T(t) \right\rangle \tag{20}$$

Let

$$Q = \left\langle \phi(t), \phi^T(t) \right\rangle = [\delta_{jk}]_{j,k=0}^{n} \tag{21}$$

where $\delta_{jk} = \int_0^K L_{n,j}(t) L_{n,k}(t) dt = \begin{cases} \frac{K}{j+k+1}, j = k \\ 0, \qquad j \neq k. \end{cases}$. Q is a diagonal matrix of order $n+1$ with positive diagonal elements, So Q is reversible. Therefore

$$B^T = \left\langle w(t), \phi^T(t) \right\rangle Q^{-1} \tag{22}$$

Similarly, the continuous function $w(t)$ in the domain $[0, S]$ can be approximated as

$$w(x) \approx w_n(x) = \sum_{k=0}^{n} i_k L_{n,k}(t) = I^T \phi(x) \tag{23}$$

where $I^T = [i_0, i_1, ..., i_n]$. so

$$I^T \left\langle \phi(x), \phi^T(x) \right\rangle = \left\langle w(t), \phi^T(x) \right\rangle \tag{24}$$

Let

$$P = \left\langle \phi(x), \phi^T(x) \right\rangle = [\Delta]_{j,k=0}^{n} \tag{25}$$

where $\delta_{jk} = \int_0^S L_{n,j}(x) L_{n,k}(x) dx = \begin{cases} \frac{S}{j+k+1}, j = k \\ 0, \qquad j \neq k. \end{cases}$. P is a diagonal matrix of order $n+1$ with positive diagonal elements, So P is reversible. Therefore

$$I^T = \left\langle w(t), \phi^T(x) \right\rangle P^{-1} \tag{26}$$

Two dimensional continuous function $w(x,t) \in L^2([0,S] \times [0,K])$ is written as

$$w(x,t) \approx \sum_{j=0}^{n} \sum_{k=0}^{n} c_{jk} L_{n,j}(x) L_{n,k}(t) = \phi^T(x) C \phi(t) \tag{27}$$

where $C = [c_{jk}]_{j,k=0}^{n}$ is the matrix coefficient to be solved.

4.3. Derivation of operator matrix

4.3.1. Integer order operator matrix

The expression of the first-order derivative of $\phi(x)$ with respect to x is [41; 42].

$$\phi'(x) = (UH(x))' = UH'(x) = UPH(x) = UPU^{-1}\phi(x) = N_x \phi(x) \tag{28}$$

where $P = [p_{jk}]_{j,k=0}^{n}$, $p_{jk} = \begin{cases} j, j = k+1 \\ 0, j \neq k+1 \end{cases}$, and $N_x = UPU^{-1}$.

Therefore, the polynomial's first-order differential operator matrix is determined to be N_x.

The second-order derivative of $\phi(x)$ with relation to x is denoted by [47; 48].

$$\begin{aligned} \phi''(x) &= (UH(x))'' = U(H'(x))' = (UPU^{-1}\phi(x))' \\ &= UPU^{-1}\phi'(x) = (UPU^{-1})^2 \phi(x) = N_x^2 \phi(x) \end{aligned} \tag{29}$$

where $N_x^2 = \left(UPU^{-1}\right)^2$ is the polynomial's second-order differential operator matrix.

An array of integer order operators is derived from the obtained first-order and second-order operator matrices

$$\begin{aligned} \phi^{(m)}(x) &= (UPU^{-1})^m \phi(x) = N_x^m \phi(x) \\ \phi^{(m)}(t) &= (VPV^{-1})^m \phi(t) = N_t^m \phi(t) \end{aligned} \tag{30}$$

The differential term in Eq. (8) is written as

$$\begin{aligned} \tfrac{\partial w(x,t)}{\partial x} &\approx \tfrac{\partial(\phi^T(x) C \phi(t))}{\partial x} = \tfrac{\partial \phi^T(x)}{\partial x} C \phi(t) \\ &= \phi^T(x)(UPU^{-1}) C \phi(t) \end{aligned} \tag{31}$$

$$\begin{aligned} \tfrac{\partial^2 w(x,t)}{\partial x^2} &\approx \tfrac{\partial^2(\phi^T(x) C \phi(t))}{\partial x^2} = \tfrac{\partial^2 \phi^T(x)}{\partial x^2} C \phi(t) \\ &= \phi^T(x)(UPU^{-1})^2 C \phi(t) \end{aligned} \tag{32}$$

$$\begin{aligned} \tfrac{\partial^2 w(x,t)}{\partial t^2} &\approx \tfrac{\partial^2(\phi^T(x) C \phi(t))}{\partial t^2} = \phi^T(x) C \tfrac{\partial^2 \phi(t)}{\partial t^2} \\ &= \phi^T(x) C (VPV^{-1})^2 \phi(t) \end{aligned} \tag{33}$$

4.3.2. Fractional order

If the matrix N_t, satisfying $D_t^\alpha \phi(t)$, the following expression is obtained from [41; 42].

$$D_t^\alpha \phi(t) = D_t^\alpha (VH(t)) = VD_t^\alpha H(t) = VFH(t) \tag{34}$$

where $F = [f_{jk}]_{j,k=0}^n$, $f_{jk} = \begin{cases} \frac{\Gamma(j)}{\Gamma(j+1)} t^{-\alpha}, j = k, j \neq 1 \\ 0, \qquad\qquad otherwise. \end{cases}$

Due to $H(t) = V^{-1}\phi(t)$, $D_t^\alpha \phi(t)$ can get be expressed

$$D_t^\alpha \phi(t) = N_t \phi(t) = VFV^{-1}\phi(t) \tag{35}$$

The fractional order term in the Eq. (8) is

$$\begin{aligned} D_t^\alpha \frac{\partial^2 w(x,t)}{\partial x^2} &\approx D_t^\alpha \left[\phi^T(x)(UPU^{-1})^2 C\phi(t)\right] \\ &= \phi^T(x)(UPU^{-1})^2 C D_t^\alpha \phi(t) \\ &= \phi^T(x)(UPU^{-1})^2 CVFV^{-1}\phi(t) \end{aligned} \tag{36}$$

4.4. Transformation of the governing equation

The governing equation of the rod can be expressed by using the differential operator matrix defined previously

$$\begin{aligned} &\rho\phi^T(x)C(VPV^{-1})^2\phi(t) - E_1\phi^T(x)(UPU^{-1})^2C\phi(t) - E_2\phi^T(x)(UPU^{-1})^2CVFV^{-1}\phi(t) \\ &+c_0\rho\phi^T(x)C\phi(t) + c_1\rho(\phi^T(x)C\phi(t))^3 = f(x,t) \end{aligned} \tag{37}$$

Convert boundary conditions to

$$\begin{cases} \phi^T(0)\,C\phi(t) = 0 \\ \phi^T(l)\,C\phi(t) = 0 \end{cases} \tag{38}$$

Convert initial conditions to

$$\begin{cases} \phi^T(x)C\phi(0) = 0 \\ \phi^T(x)C(VPV^{-1})\phi(0) = 0 \end{cases} \tag{39}$$

Eq. (37) can be transformed into algebraic equations, in which the coefficient matrix are identified by using the least square method.

5. Convergence analysis and dimensionless equation

5.1. Convergence analysis

$w(t)$ is a sufficiently smooth function on $[0, K]$, $q_n(t)$ is the interpolation polynomial of w at t_i, t_i $(n = 0, 1, ..., n)$ is the root of $n+1$ degree Chebyshev polynomial at $[0, K]$, then there is

$$w(t) - q_n(t) = \frac{w^{(n+1)}(\xi)}{(n+1)!} \prod_{i=0}^{n} (t - t_i), \quad \xi \in [0, K] \tag{40}$$

Therefore, it can be obtained

$$|w(t) - q_n(t)| \leq \frac{A_n (K)^{n+1}}{2^{2n+1}(n+1)!} \tag{41}$$

where$A_n = \max_{0 \leq t \leq K} \left| w^{(n+1)}(t) \right|$.

Theorem 1. Suppose $w(t)$ is a continuous differentiable function,$w_n(t) = D^T \phi(t)$ is the shifted Legendre polynomials expansion of the exact solution $w(t)$, $D = [d_0, d_1, ...d_n], \phi(t) = [\phi_0(t), \phi_1(t), ...\phi_n(t)]$.

Let $\bar{w}_n(t) = \sum\limits_{i=0}^{n} \bar{a}_i \phi_i(t)$ be an approximate solution, there are real numbers λ and μ, such that

$$\|w(t) - \bar{w}_n(t)\|_2 \leq \lambda \frac{A_n (K)^{n+1}}{2^{2n+1}(n+1)!} + \mu \left\| D - \bar{D} \right\|_2 \tag{42}$$

The norm on the right is the Euclidean norm of a vector.

Proof. $R[t]$ is a space of real-valued polynomials of order $\leq n$, $w_n(t)$ and $\bar{w}_n(t)$ are in space $R[t]$, $\bar{w}_n(t)$ is the best approximation of $w(t)$.

$$\|w(t) - \bar{w}_n(t)\|_2 \leq \|w(t) - w_n(t)\|_2 + \|w_n(t) - \bar{w}_n(t)\|_2 \tag{43}$$

According to Eq. (41), we can get

$$\begin{aligned} \|w(t) - w_n(t)\|_2 &= \left(\int_0^K |w(t) - w_n(t)|^2 dt \right)^{\frac{1}{2}} \\ &\leq \left(\int_0^K \left[\tfrac{A_n (K)^{n+1}}{2^{2n+1}(n+1)!} \right]^2 dt \right)^{\frac{1}{2}} \\ &\leq \sqrt{K} \tfrac{A_n (K)^{n+1}}{2^{2n+1}(n+1)!} \end{aligned} \tag{44}$$

Then

$$
\begin{aligned}
\left\|w_n(t)-\bar{w}_n(t)\right\|_2 &= \left(\int_0^K\left[\sum_{i=0}^{n}\left(d_i-\bar{d}_i\right)\phi_i(t)\right]^2 dt\right)^{\frac{1}{2}} \\
&\leq \left(\int_0^K\left[\sum_{i=0}^{n}\left|d_i-\bar{d}_i\right|^2\right]\left[\sum_{i=0}^{n}\left|\phi_i(t)\right|^2 dt\right]\right)^{\frac{1}{2}} \\
&= \left[\sum_{i=0}^{n}\left|d_i-\bar{d}_i\right|^2\right]^{\frac{1}{2}}\left(\sum_{i=0}^{n}\int_0^K\left|\phi_i(t)\right|^2 dt\right)^{\frac{1}{2}} \\
&= \left\|D-\bar{D}\right\|_2\left(K\sum_{i=0}^{n}\frac{1}{2i+1}\right)^{\frac{1}{2}}
\end{aligned}
\tag{45}
$$

So $\lambda=\sqrt{K}, \mu=\sqrt{K\left(\sum_{i=0}^{n}\frac{1}{2i+1}\right)}$.

The above theorem is proved.

5.2. Dimensionless equation

The structure of the dimensionless equation is consistent with the governing equation of nonlinear viscoelastic rod (Eq. (8)). The shifted Legendre polynomials algorithm is used to determine the numerical solution. The coefficients in the equation are dimensionless. Its analytical solution is known and it is used to verify the accuracy of the proposed algorithm.

The dimensionless equation is expressed as

$$
600\frac{\partial^2 w(x,t)}{\partial t^2}-\frac{\partial^2 w(x,t)}{\partial x^2}-D_t^{\alpha}\frac{\partial^2 w(x,t)}{\partial x^2}+100000w(x,t)+w^3(x,t)=f(x,t) \tag{46}
$$

These are the boundary conditions

$$
w(0,t)=w(1,t)=0 \tag{47}
$$

where $\alpha=0.35$, the exact solution of Eq. (46) is $w(x,t)=x^3(1-x)^3t^2$.

Substitute the exact solution into Eq. (46), and we get

$$
\begin{aligned}
f(x,t) &= 1200x^3(1-x)^3-6[x^3(1-x)-3x^2(1-x)^2+x(1-x)^3]t^2 \\
&\quad -6[x^3(1-x)-3x^2(1-x)^2+x(1-x)^3]\tfrac{\Gamma(3)}{\Gamma(3-\alpha)}t^{2-\alpha} \\
&\quad +100000x^3(1-x)^3t^2+[x^3(1-x)^3t^2]^3
\end{aligned}
\tag{48}
$$

The shifted Legendre polynomials algorithm is applied to solve the differential governing equation at $n=6$, the exact solution and numerical solution are denoted by $w(x,t)$ and $w_n(x,t)$, respectively. The numerical solution is essentially consistent with the analytical solution, as illustrated in Fig. 2. The absolute error is $e_n = |w_n(x,t) - w(x,t)|$.

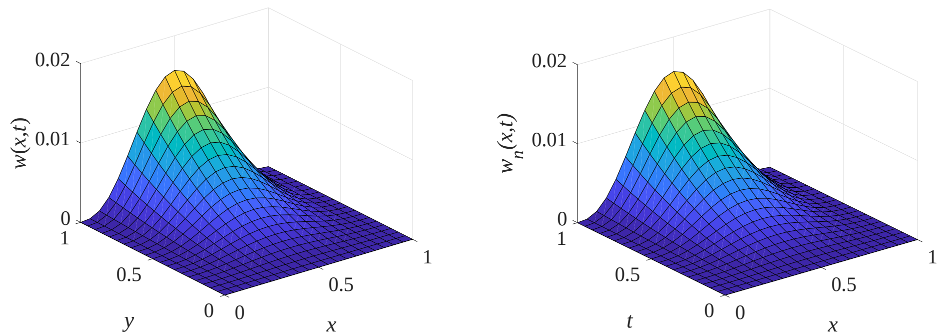

(a) exact solution (b) numerical solution

Fig. 2. $n = 6$, numerical solution and exact solution at different points.

As can be clearly seen from Fig. 3, an increase in the number of terms n leads to a gradual decrease in absolute error and a higher accuracy of the numerical solution. The validity and accuracy of the shifted Legendre polynomial algorithm are proved. It is further demonstrated that the algorithm is an effective algorithm for analyzing the dynamic characteristics of fractional order viscoelastic rod. Therefore, the following dynamic analysis of a viscoelastic material rod retains $n = 6$ for calculation.

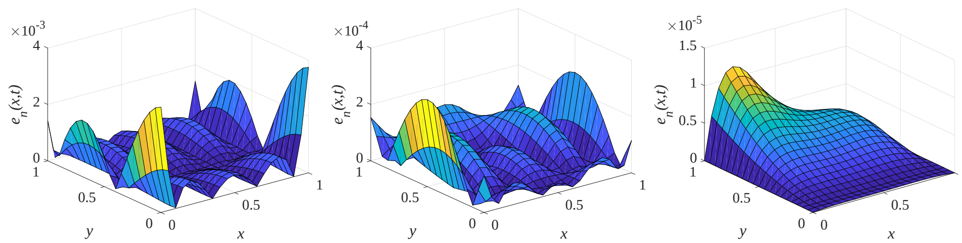

(a) $n = 4$ (b) $n = 5$ (c) $n = 6$

Fig. 3. Absolute error when n is different.

6. Dynamic analysis

In this part, the dynamic characteristics of nonlinear viscoelastic rod are examined using the shifted Legendre algorithm.

The geometrical characteristics and material properties of viscoelastic rod are shown in the following Tab. 1 [23], calculation by assumption $c_0 = 1.34 \times 10^{-4} s^{-2}$ and $c_1 = 1.34 \times 10^{-4} m^{-2} s^{-2}$.

Table 1: Geometrical characteristics and material properties of viscoelastic rod.

Physical quantity	Symbol	Value	Unit
Length	l	1	m
Cross-sectional area	A	1	m^2
Density	ρ	7500	$\mathrm{kg/m}^3$
Instant elasticity modulus	E_1	2×10^{11}	Pa
Prolonged elasticity modulus	E_2	2×10^{11}	Pa s^{α}

6.1. *The effect of uniformly distributed axial load*

The fractional order viscoelastic rod differential equation is directly derived in the time domain using the shifted Legendre algorithm. The numerical solutions of displacement for various uniformly distributed axial load, at different times and locations, are shown in Fig. 4.

As shown in Fig. 4, when uniformly distributed axial load of different magnitudes are applied to the viscoelastic rod, the displacement at both ends of the rod is always zero, independent of time, and conforms to the boundary conditions. The displacement of the viscoelastic rod is the largest at 0.5 m, and the displacement change is symmetric about $x = 0.5$ m. The displacement of the rod increases with applied uniform load. When the same uniform load is applied, the displacement will increase with loading time.

6.2. *The effect of linearly distributed load*

Apply linear loads to the viscoelastic rod, such as $f = ax + b$. Fig. 5 shows the numerical displacement solutions at the time of $t = 0.5$ s and $t = 1$ s when the

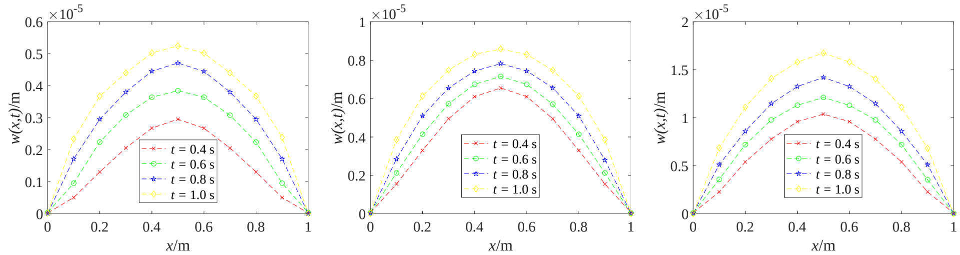

(a) $f = 5$ N/m^3 (b) $f = 10$ N/m^3 (c) $f = 15$ N/m^3

Fig. 4. The displacement change of the rod under different uniformly distributed axial load.

viscoelastic rod is subjected to the various linear loads.

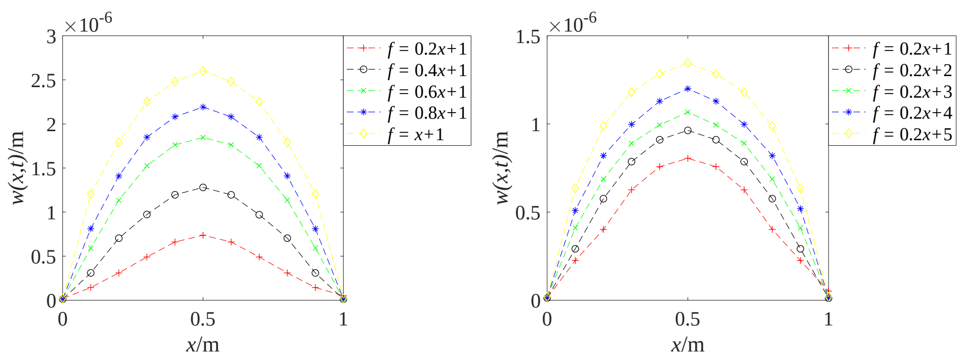

(a) $t = 0.5$ s (b) $t = 1$ s

Fig. 5. Displacement of the rod under different linearly distributed load.

Fig. 5 clearly shows that the evolution of the displacement of viscoelastic rod under linear load is consistent, which is symmetrical in the middle, and reaches the maximum value at $x = 0.5$ m. The displacement of viscoelastic rod is related to a and b in the linear loads. In Fig. 5(a), b is fixed as constant 1, and when a rises, the displacement increases as well.; in Fig. 5(b), a is fixed as constant 0.2, and the displacement also increases with the increase of b. The numerical calculation results are in good agreement with the actual observation results, which verifies the efficiency of the algorithm.

6.3. The effect of harmonic load

The viscoelastic rod is subjected to a harmonic load in the form of $f = A\cos(Bt)$, A and B are amplitude and frequency respectively. The displacement changes of the viscoelastic rod under different harmonic loads and different times are shown in Fig. 6.

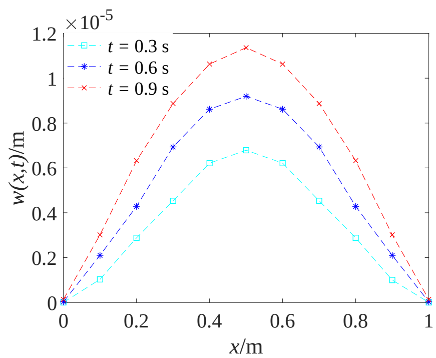

(a) $f = 10\cos(0.01t)$

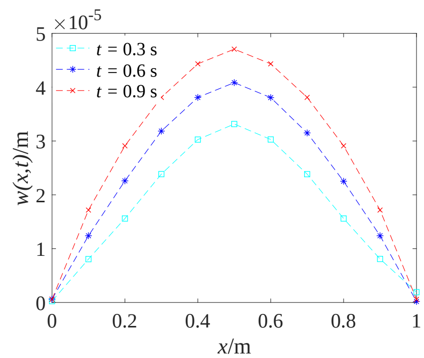

(b) $f = 50\cos(0.01t)$

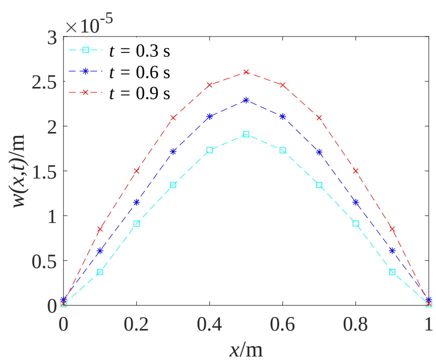

(c) $f = 50\cos(0.05t)$

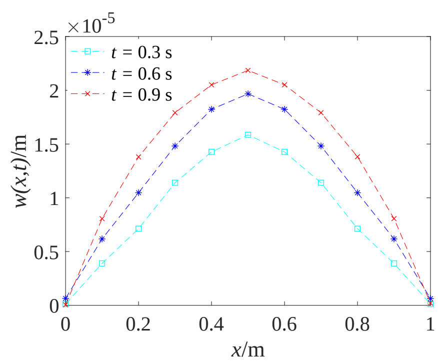

(d) $f = 50\cos(0.1t)$

Fig. 6. Displacement of the rod under different simple harmonic loads.

It can be clearly seen from Fig. 6 that harmonic load is applied to the viscoelastic rod, and the change of displacement is basically zero at both ends of the rod and reaches the maximum value in the middle of the rod. When the viscoelastic rod is subjected to the same load, as the amount of time increases, the rod's displacement will also rise. When the viscoelastic rod is exposed to various harmonic loads, the displacement of the rod will rise with an increase in A when B is fixed, and decrease with an increase in B when A is fixed.

6.4. The evolution of stress under uniformly distributed axial load

Eq. (6) states that by using the algorithm, the numerical solution of stress can be obtained. The stress values of viscoelastic rods under uniformly distributed axial load are shown in Fig. 7.

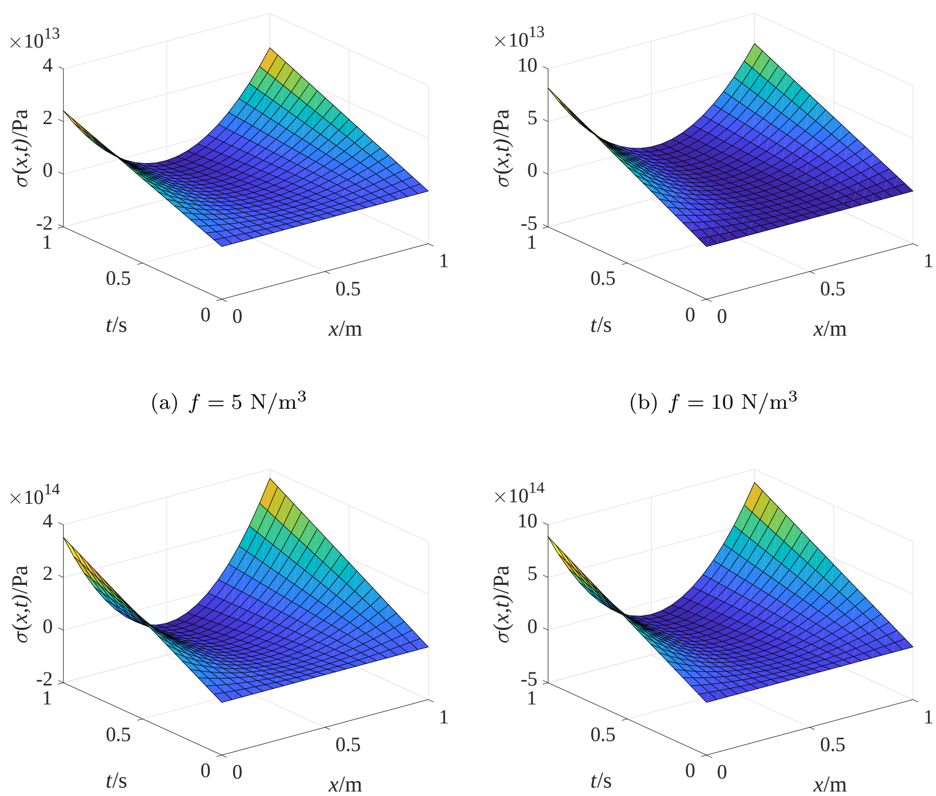

(a) $f = 5$ N/m^3 (b) $f = 10$ N/m^3

(c) $f = 15$ N/m^3 (d) $f = 20$ N/m^3

Fig. 7. Stress of the rod under different values of uniformly distributed load.

The stress variation diagram of viscoelastic rod subjected to different uniformly distributed axial load can be clearly seen in Fig. 7. The stress value is also symmetrical about $x = 0.5$ m. The stress value is zero when the loading time is 0.

At the same loading time, the rod has the highest stress value at both ends. The displacement of the rod increases with value of uniformly distributed load. The value of stress in the middle of the rod is smallest, which is consistent with the evolution of the displacement.

7. Conclusions

The fractional differential governing equation of the nonlinear viscoelastic rod is established by using the fractional order constitutive model. An effective numerical algorithm based on the shifted Legendre polynomials is proposed to solve directly the fractional governing equation in the time domain. The convergence analysis is performed to validate the proposed method and confirm its efficiency. The numerical solution of the displacement of the viscoelastic rod is obtained under various external loading conditions.

1. The fractional order behavior law is successfully implemented in the governing equation of the nonlinear rod to take into account the viscoelasticity of the material.

2. When the uniformly distributed axial load and linearly distributed axial load are applied on the rod, the displacement increases with the value of the load and time.

3. The displacement of the rod increases with time, when the simple harmonic load is applied. The displacement increases with the amplitude of the load and decreases with the frequency.

4. The stress of the viscoelastic rod under different values of uniformly distributed axial load is calculated. The maximum value of stress is at the ends of rod and the minimum value is in the middle of the rod.

Declaration of competing interest

The authors declare that they have no known competing economic interests or personal relationships that may affect the work in this article.

Acknowledgements

This work is supported by National Natural Science Foundation of China (5207041692) and the LE STUDIUM RESEARCH PROFESSORSHIP award of Centre-Val de Loire region in France.

References

[1] A.G. Cunha-Filho, A.M.G.D. Lima, M.V. Donadon, L.S. Leão, Flutter suppression of plates using passive constrained viscoelastic layers, Mech Syst Signal Pr. 79 (2016) 99–11, https://doi.org/10.1016/j.ymssp.2016.02.025.

[2] P.C.O. Martins, T.A.M. Guimarães, D.D A. Pereira, F.D. Marques, F.A. Rade, Numerical and experimental investigation of aeroviscoelastic systems, Mech Syst Signal Pr. 85 (2017) 680–697, https://doi.org/10.1016/j.ymssp.2016.08.043.

[3] A.M.G. Lima, D.A. Rade, H.B. Lacerda, C.A. Araújo, An investigation of the self-heating phenomenon in viscoelastic materials subjected to cyclic loadings accounting for prestress, Mech Syst Signal Pr. 58-59 (2015) 115–127, https://doi.org/10.1016/j.ymssp.2014.12.006.

[4] S. Sepehr Tabatabaei, R.D. Mohammad, Modeling and adaptive identification of arterial behavior;a variableorder approach, J Comput Sci-Neth. 62 (2022) 101691, https://doi.org/10.1016/j.jocs.2022.101691.

[5] J. Yang, Daniel Custer, C.C. Chiang, Z.X. Meng, X.H. Yao, Understanding the mechanical and viscoelastic properties of graphene reinforced polycarbonate nanocomposites using coarse-grained molecular dynamics simulations, Comp Mater Sci. 191 (2021) 110339, https://doi.org/10.1016/j.commatsci.2021.110339.

[6] M. Viktorova, R. Hentschke, F. Fleck, F. Taherian, H.A. Karimi-Varzaneh, A mesoscopic model for the simulation of dynamic mechanical properties of filled elastomers:Filled binary polymer blends, Comp Mater Sci. 212 (2022) 111597, https://doi.org/10.1016/j.commatsci.2022.111597.

[7] N. Jiang, Y.Q. Feng, X.J. Wang, Fractional-order evolutionary game of green and low-carbon innovation in manufacturing enterprises, Alex Eng J. 61 (2022) 12673C12687, https://doi.org/10.1016/j.aej.2022.06.040.

[8] I. Birs, I. Nascu, C. Ionescu, C. Muresan, Event-based fractional order control, J Adv Res. 25 (2020) 191–203, https://doi.org/10.1016/j.jare.2020.06.024.

[9] Y.H. Wei, Q. Gao, On the series representation of nabla discrete fractional calculus, Comput Math Appl. 430 (6) (2022) 127303, https://doi.org/10.1016/j.ijnonlinmec.2017.11.010.

[10] H.Y. Xu, X.Y. Jiang. , Creep constitutive models for viscoelastic materials based on fractional derivatives, Comput Math Appl. 73 (2017) 1377–1384, https://doi.org/10.1016/j.camwa.2016.05.002.

[11] M.A. Ezzat, A.S. El-Karamany, A.A. El-Bary, M.A. Fayik, Fractional calculus in one-dimensional isotropic thermo-viscoelasticity, C R Mecanique. 341 (2013) 553C566, https://doi.org/10.1016/j.crme.2013.04.001.

[12] E. Loghman, F. Bakhtiari-Nejad, E.A. Kamali, M. Abbaszadeh, Nonlinear random vibrations of micro-beams with fractional viscoelastic core, Probabilist Eng Mech. 69 (2022) 103274, https://doi.org/10.1016/j.probengmech.2022.103274.

[13] A. Ouzizi, F. Abdoun, L. Azrar, Nonlinear dynamics of beams on nonlinear fractional viscoelastic foundation subjected to moving load with variable speed, J Sound Vib. 523 (2022) 116730, https://doi.org/10.1016/j.jsv.2021.116730.

[14] Y.F. Gao, D.S. Yin, A full-stage creep model for rocks based on the variable-order fractional calculus, Appl Math Model. 95 (2021) 435–446, https://doi.org/10.1016/j.apm.2021.02.020.

[15] Y. Denis, F. Morestin , N. Hamila, A hysteretic model for fiber-reinforced composites at finite strains: fractional derivatives, computational aspects and analysis, Comp Mater Sci. 181 (2020) 109716, https://doi.org/10.1016/j.commatsci.2020.109716.

[16] E. Loghman , F. Bakhtiari-Nejad, K. E. Ali , M. Abbaszadeh, M. Amabili, Nonlinear vibration of fractional viscoelastic micro-beams, Int J Nonlin Mech. 137 (2021) 103811, https://doi.org/10.1016/j.ijnonlinmec.2021.103811.

[17] X. Liu, Y.X. Zhao, W. Zhou, J.R. Banerjee, Dynamic stiffness method for exact longitudinal free vibration of rods and trusses using simple and advanced theories, Appl Math Model. 104 (2022) 401–420, https://doi.org/10.1016/j.apm.2021.11.023.

[18] H. Lang, M. Arnold, Numerical aspects in the dynamic simulation of geometrically exact rods, Appl Numer Math. 62 (2012) 1411–1427, https://doi.org/10.1016/j.apnum.2012.06.011.

[19] I.V. Kudinov, A.V. Eremin, V.A. Kudinov, A.I. Dovgyallo, V.V. Zhukov, Mathematical model of damped elastic rod oscillations with dual-phase-lag, Int J Solids Struct. 200-201 (2020) 231–241, https://doi.org/10.1016/j.ijsolstr.2020.05.018.

[20] A.T. Alp, N.A. Reshad, T. Beytullah, Dynamic response of viscoelastic tapered cycloidal rods, Mech Res Commun. 92 (2018) 8–14, https://doi.org/10.1016/j.mechrescom.2018.06.006.

[21] S. Adhikari, T. Murmu, M.A. Mccarthy, Dynamic finite element analysis of axially vibrating nonlocal rods, Finite Elem Anal Des. 63 (2013) 42–50, https://doi.org/10.1016/j.finel.2012.08.001.

[22] K. Mazur-Śniady, P. Śniady., W. Zielichowski-Haber, Dynamic response of micro-periodic composite rods with uncertain parameters under moving random load, J Sound Vib. 320 (1-2) (2009) 273–288, https://doi.org/10.1016/j.apm.2019.12.011.

[23] G. Malara, B. Pomaro, P.D. Spanos, Nonlinear stochastic vibration of a variable cross-section rod with a fractional derivative element, Int J Nonlin Mech. 135 (2021) 103770, https://doi.org/10.1016/j.ijnonlinmec.2021.103770.

[24] H.W. Du, Q.W. Jiang, W. Xiong, Unified static equilibrium modeling and analysis of elastic rods with large deformations for complex constraints, Commun Nonlinear Sci. 113 (2022) 106583, https://doi.org/10.1016/j.cnsns.2022.106583.

[25] R.F. Ausas, C.G. Gebhardt, G.C. Buscaglia, A finite element method for simulating soft active non-shearable rods immersed in generalized Newtonian fluids, Commun Nonlinear Sci. 108 (2022) 106213, https://doi.org/10.1016/j.cnsns.2022.106213.

[26] Y.P.Zhang, Axial vibration analysis of nanorods with variable density based on nonlocal elastic theory and high-order finite difference method, J Comput Sci-Neth. 55 (2021) 101452, https://doi.org/10.1016/j.jocs.2021.101452.

[27] S.J. Shakhlavi, On nonlinear damping effects with nonlinear temperature-dependent properties for an axial thermo-viscoelastic rod, Int J Nonlin Mech. 153 (2023) 104418, https://doi.org/10.1016/j.ijnonlinmec.2023.104418.

[28] N. Li, M.T. Yan, Bifurcation control of a delayed fractional-order prey-predator model with cannibalism and disease, Chaos Soliton Fract. 600 (2022) 127600, https://doi.org/10.1016/j.physa.2022.127600.

[29] S. Maiti, S. Shaw, G.C. Shit, Fractional order model of thermo-solutal and magnetic nanoparticles transport for drug delivery applications, Colloid Surface B. 203 (2021) 40–54, https://doi.org/10.1016/j.colsurfb.2021.111754.

[30] B.B. Zheng, Z.S. Wang, Mittag-Leffler synchronization of fractional-order coupled neural networks with mixed delays, Appl Math Comput. 430 (2022) 127303, (https://doi.org/10.1016/j.amc.2022.127303.

[31] S. Al-Nassir, Dynamic analysis of a harvested fractional-order biological system with its discretization, Chaos Soliton Fract. 152 (2021) 111308, https://doi.org/10.1016/j.chaos.2021.111308.

[32] S. Patnaik, S. Sidhardh, F. Semperlotti, Fractional-Order models for the static and dynamic analysis of nonlocal plates, Commun Nonlinear Sci. 95 (2021) 105601, https://doi.org/10.1016/j.cnsns.2020.105601.

[33] T.P. Stefański, On possible applications of media described by fractional-order models in electromagnetic cloaking, Commun Nonlinear Sci. 99 (2021) 105827, https://doi.org/10.1016/j.cnsns.2021.105827.

[34] M. Javadi, M. Rahmanian, Nonlinear vibration of fractional Kelvin-Voigt viscoelastic beam on nonlinear elastic foundation, Commun Nonlinear Sci. 98 (2021) 105784, https://doi.org/10.1016/j.cnsns.2021.105784.

[35] J.W. Cao, Y.M. Chen, Y.H. Wang, T. Barriére, L. Wang, Numerical analysis of fractional viscoelastic column based on shifted Chebyshev wavelet function, Appl Math Model. 91 (2021) 374–389, https://doi.org/10.1016/j.apm.2020.09.055.

[36] R.Q. Dang, Y.M. Chen, Fractional modelling and numerical simulations of variable-section viscoelastic arches, Appl Math Comput. 409 (22) (2021) 126376, https://doi.org/10.1016/j.amc.2021.126376.

[37] L. Sun, Y.M. Chen, R.Q. Dang, G. Cheng, J.Q. Xie, Shifted legendre polynomials algorithm used for the numerical analysis of viscoelastic plate with a fractional order model, Math Comput Simulat. 193 (2022) 190–203, https://doi.org/10.1016/j.matcom.2021.10.007.

[38] G.H. Ibraheem, M. Turkyilmazoglu, M.A. AL-Jawary, Novel approximate solution for fractional differential equations by the optimal variational iteration method, J Comput Sci-Neth. 64 (2022) 101841, https://doi.org/10.1016/j.jocs.2022.101841.

[39] M. Usman, W. Alhejaili, M. Hamid, N. Khan, Fractional analysis of jeffrey fluid over a vertical plate with time-dependent conductivity and diffusivity: A low-cost spectral approach, J Comput Sci-Neth. 63 (2022) 101769, https://doi.org/10.1016/j.jocs.2022.101769.

[40] M.H. Heydari, M. Razzaghi, D. Baleanu, Numerical solution of distributed-order time fractional KleincGordoncZakharov system, J Comput Sci-Neth. 67 (2023) 101961, https://doi.org/10.1016/j.jocs.2023.101961.

[41] M.H. Heydari, Z. Avazzadeh, A. Atangana, Orthonormal shifted discrete Legendre polynomials for solving a coupled system of nonlinear variable-order time fractional reaction-advection-diffusion equations, Appl Numer Math. 161 (2) (2021) 425–436, https://doi.org/10.1016/j.apnum.2020.11.020.

[42] J.W. Cao, Y.M. Chen, Y.H. Wang, G. Cheng, B. Thierry, Shifted Legendre polynomials algorithm used for the dynamic analysis of PMMA viscoelastic beam with an improved fractional model, Chaos Soliton Fract. 141 (2020) 110342, https://doi.org/10.1016/j.chaos.2020.110342.

[43] E. Hesameddini, M. Shahbazi, Two-dimensional shifted Legendre polynomials operational matrix method for solving the two-dimensional integral equations of fractional order, Appl Math Comput. 322 (2018) 40–54, https://doi.org/10.1016/j.amc.2017.11.024.

[44] M. Hosseininia, M.H. Heydari, Z. Avazzadeh, Orthonormal shifted discrete Legendre polynomials for the variable-order fractional extended Fisher-Kolmogorov equation, Chaos Soliton Fract. 155 (2022) 111729, https://doi.org/10.1016/j.chaos.2021.111729.

[45] C.X. Yu, J. Zhang, Y.M. Chen, Y.J. Feng, A.M. Yang, A numerical method for solving fractional-order viscoelastic EulercBernoulli beams, Chaos Soliton Fract. 128 (2019) 275–279, https://doi.org/10.1016/j.chaos.2019.07.035.

[46] L. Sun, Y.M. Chen, Numerical analysis of variable fractional viscoelastic column based on two-dimensional Legendre wavelets algorithm, Chaos Soliton Fract. 152 (2021) 111372, https://doi.org/10.1016/j.chaos.2021.111372.

[47] C.D. Han, Y.M. Chen, D.Y. Liu, D. Boutat, Numerical analysis of viscoelastic rotating beam with variable fractional order model using shifted BernsteincLegendre polynomial collocation algorithm, Fractal Fract. 5 (2021) 8, https://doi.org/10.3390/fractalfract5010008.

[48] Y.H. Wang, Y.M. Chen, Shifted Legendre Polynomials algorithm used for the dynamic analysis of viscoelastic pipes conveying fluid with vari-

able fractional order model, Appl Math Model. 81 (2020) 159–176, https://doi.org/10.1016/j.apm.2019.12.011.